ISBN: 978-3-95450-247-9 ISSN: 2673-5490 doi: 10.18429/JACoW-IPAC2024-THPS44

DIFFUSION BONDING OF TUNGSTEN-VANADIUM-ZIRCONIUM USING VACUUM HOT PRESSING FOR THE DEVELOPMENT OF A LOW DECAY HEAT CLADDING SOLUTION FOR TUNGSTEN SPALLATION TARGETS*

Y. Lee†, T. Muth, J. Mach and J. Montross
Oak Ridge National Laboratory, Oak Ridge, Tennessee, USA

Abstract

Tantalum has been used as cladding material for water-cooled solid tungsten targets at many leading spallation neutron production facilities thanks to its high neutron yield, manageable radiation damage behavior, and excellent corrosion/erosion resistance in radiation environments. However, from a safety hazard perspective, thermal neutron capture of tantalum in spallation environments causes a high specific decay heat in the target volume, which often becomes a limiting factor in increasing the beam power on the target. In this paper, we studied vacuum hot pressing (VHP) parameters to diffusion bond zirconium to tungsten to explore the feasibility of using zirconium alloys as an alternative cladding material to tantalum. Zirconium alloys have long been used as cladding material for early generation solid spallation targets, and nuclear fuel rods. In spallation environments zirconium has significantly lower decay heat with shorter decay time compared to tantalum. The hot isostatic pressing (HIP) of zirconium and tungsten is known to produce limited bonding quality due to the formation of the brittle ZrW_2 intermetallic layer. To overcome this problem, placing a vanadium interlayer between tungsten and zirconium has been proposed by exploring parameter space in binary alloy phase diagrams. Under the VHP conditions, 860 °C at 70 MPa for 4 hours, Zr-V and V-W showed good diffusion bonding, which demonstrates the feasibility of a single step HIP process to make the zirconium alloy clad tungsten spallation volumes.

INTRODUCTION

Tantalum has been used as cladding material for water-cooled solid tungsten targets at high-power spallation neutron production facilities which include LANSCE at LANL [1], TS1 and TS2 at ISIS [2], and at CSNS [3]. Tantalum has high neutron yield thanks to its high nuclei density. It has shown manageable radiation damage behavior as demonstrated in post-irradiation-examination (PIE) of tantalum irradiated at ISIS [4] and at PSI [5], showing moderate ductility at high displacement doses and excellent corrosion/erosion resistance in radiation environments. However, thermal neutron capture of ^{181}Ta in a spallation environment produces ^{182}Ta, which causes a high specific decay heat in the target volume with a 114.4 day long decay time. Due to its high specific decay heat the second-generation ISIS targets made of pure tantalum suffered from high tritium release during end of life storage [6]. In conceptualization of next generation high power solid tungsten targets, the high decay heat from tantalum clad volume is a limiting factor in increasing the beam power on the target. A study shows that the proton beam power higher than 400 kW on a tantalum clad tungsten target could induce the maximum temperature in the tungsten volume exceeding 800 °C [7] in loss of coolant accidents (LOCA). Above 800 °C in steam environment, tungsten oxidizes aggressively and becomes airborne [8], posing radiological safety hazards.

Zirconium alloys have long been used as cladding material for early generation solid spallation targets at KENS [9], IPNS [10] and ISIS [2] and for canning material at PSI lead target [11], and it has been widely used as a cladding material for nuclear fuel rods. It causes significantly lower specific decay heat with shorter decay time compared to tantalum in spallation environments. However, the technology to diffusion bond zirconium alloys to tungsten has not been fully explored, which is required for a successful development of a zirconium alloy clad tungsten target subject to a high proton beam power.

Hot Isostatic Pressing (HIP) of zirconium cladding on tungsten has been studied in Ref. [12] for a peak pressure of 180 MPa kept at 1200 °C, 1300 °C and 1400 °C for 4 hours. The depth of diffusion layer was 6–13 μm, which increased with the HIP temperature. At a different HIP condition with a peak pressure of 100 MPa kept at 900 °C for 1.5 hours followed by 70 MPa kept at 750 °C for 2 hours formed a 150 μm thick interlayer between W and Zr [13]. The measured W to Zr ratio of nearly 2 suggested the formation of a ZrW_2 intermetallic phase. Recent studies on the interdiffusion behavior of the Zr-W binary systems for the temperature range from 1300 °C to 1500 °C showed that the ZrW_2 intermetallic phase was formed in the diffused region with its layer thickness growing with temperature in accordance with the Arrhenius relationship [14]. It can be read from the Zr-W binary alloy equilibrium diagram that ZrW_2 is the only intermetallic phase. The formation of the brittle ZrW_2 intermetallic layer creates a weakness where stresses, due to differential heating and cooling, coupled with significant differences in thermal expansion coefficients, create a delamination at the bond line, which results in reduced fracture

* Notice: This manuscript has been authored by UT-Battelle, LLC, under contract DE-AC05-00OR22725 with the US Department of Energy (DOE). The US government retains and the publisher, by accepting the article for publication, acknowledges that the US government retains a nonexclusive, paid-up, irrevocable, worldwide license to publish or reproduce the published form of this manuscript, or allow others to do so, for US government purposes. DOE will provide public access to these results of federally sponsored research in accordance with the DOE Public Access Plan (https://www.energy.gov/doe-public-access-plan).
† leey1@ornl.gov

Content from this work may be used under the terms of the CC BY 4.0 licence (© 2024). Any distribution of this work must maintain attribution to the author(s), title of the work, publisher, and DOI.

ISBN: 978-3-95450-247-9 ISSN: 2673-5490 doi: 10.18429/JACoW-IPAC2024-THPS44

© Content from this work may be used under the terms of the CC BY 4.0 licence (© 2024). Any distribution of this work must maintain attribution to the author(s), title of the work, publisher, and DOI.

toughness and fatigue life of a zirconium alloy clad tungsten target that is subject to intensive proton beam pulses.

In principle, to avoid the formation of the brittle interlayer, the parameter space at both ends of the W-Zr binary alloy phase diagram could be explored, where W and Zr form a solid solution. However, this requires a HIP temperature above 1400 °C where tungsten recrystallizes and becomes brittle. At this high temperature significant grain growth in the zirconium alloys would be expected. To overcome this problem, we explored the feasibility of placing a vanadium interlayer between tungsten and zirconium. If vanadium is used as an intermediate layer the ideal processing window is predicted in the temperature range between 840 °C and 860 °C for the V-Zr bonding. The justification for this processing window is to stay below the β transus for zirconium at 863 °C but be sufficiently high in temperature to create diffusion between W and V in a reasonable time. If we process above zirconium's β transus then we would be prone to grain growth in the vanadium and to the formation of the ZrV_2 intermetallic when cooled below the β transus. On the other hand, the V-W phase diagram shows V-W solid solution region for a temperature below 1910 °C.

In this paper, we present the vacuum hot processing (VHP) process to diffusion bond zirconium to vanadium and vanadium to tungsten and evaluate the microscopic characteristics of bonding qualities. This is to explore the feasibility of using zirconium alloys as an alternative cladding material to tantalum.

EXPERIMENTAL PROCEDURE

VHP Samples

A pure tungsten coupon with a dimension of 63.5 mm × 25.5 mm × 6.0 mm was cut from a 48 mm thick forged plate purchased from Plansee SE. A zirconium coupon with dimension 63.5 mm × 25.5 mm × 1.0 mm was cut from a 1 mm thick rolled plate. A vanadium coupon with a dimension of 63.5 mm × 25.5 mm × 1 mm was cut from a 1 mm thick rolled plate. The bonding surfaces of each material were prepared by using an ethyl alcohol plus 70 µm diamond abrasive slurry to remove native oxide just prior to the thermal cycle. The slurry was manually rubbed on the mating surfaces until a fresh surface was observed.

VHP Setup

The VHP setup is schematically described in Fig. 1. The Zr, V and W coupons were stacked on top each other. On top of the tungsten coupon, a ceramic (Al_2O_3) coupon was placed. These four coupons were wrapped in a Zr-foil that works as gas getter. The Zr wrapped VHP specimen was placed on a W plate coated with Y_2O_3 which was mounted on the graphite ram. On top of the Zr getter foil, Y_2O_3 coated graphite plate was placed.

VHP Parameters

The thermal mechanical process performed in the vacuum hot press to create the W-V and V-Zr bonds was a vacuum level of $< 2 \cdot 10^{-4}$ torr with an applied bonding pressure of 70 MPa at 860 °C. The bonding cycle temperature was maintained for 4 hours for both W/V and V/Zr bonding.

Figure 1: The VHP setup used for the study.

RESULTS AND DISCUSSIONS

Metallography

Figure 2 shows the sample assembly removed after the VHP process as wrapped with zirconium getter. The Zr getter adhered to the Zr coupons exhibiting Zr to Zr bonding under the applied VHP conditions. The W, V and Zr coupons are bonded to each other with a slight bow. This was because the fracture of graphite platen occurred during the VHP procedure.

Figure 2: Sample assembly removed after the VHP process as wrapped with zirconium getter.

The bonded specimen was cut with a diamond bandsaw and the cut cross section was ground and polished. Figure 3 shows the optical metallographic image of the cut cross section at 200x magnification. Large grain structure of W typical of the large forging where the plate originated, as well as a 50 µm grain size of both the Zr and V were observed. A metallographic image of the interface area between W and V is shown in Fig. 4. At 1000x magnification on the top the diffusion zone is observed where V moved into the W. A metallographic image of the interface area between V and Zr is shown in Fig. 5. The bonding area width is between 2 and 5 µm.

Scanning Electron Microscopy

Figure 6 (top) shows the scanning electron microscopic (SEM) image of the interface area between V and Zr. The

ISBN: 978-3-95450-247-9 ISSN: 2673-5490 doi: 10.18429/JACoW-IPAC2024-THPS44

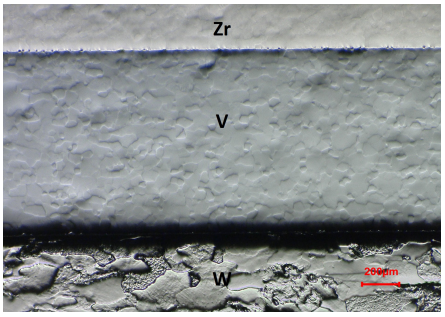

Figure 3: Metallography image of the cut cross section at 200x magnification.

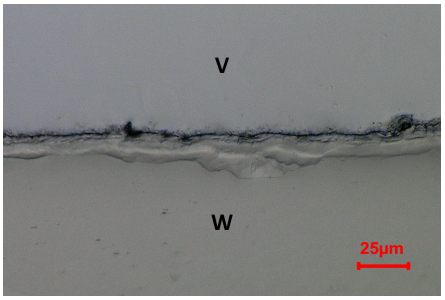

Figure 4: Metallographic image of interface area between W and V at 1000x magnification.

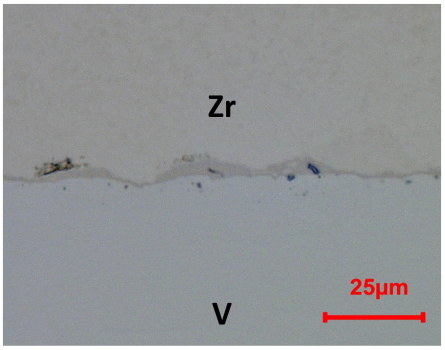

Figure 5: Metallographic image of interface area between V and Zr.

bond line between the Zr and V was found to be approximately 2.5 µm wide as measured in the SEM using a combined energy dispersive spectroscopy (EDS) line scan as shown in the figure (top). An elemental dot map was also produced as shown in figure 6 (bottom) showing the diffusion zone to be approximately a 1:1 ratio of zirconium to vanadium, indicating solid solution with the absence of the ZrV_2 intermetallic.

Figure 7 shows the SEM image of the interface area between V and W. The W-V bonding region shows about 1 µm of diffusion depth.

CONCLUSIONS

Vacuum hot pressing (VHP) of tungsten, vanadium and zirconium plates was performed to form diffusion bonding. During VHP, maximum temperature 860 °C under 70 MPa

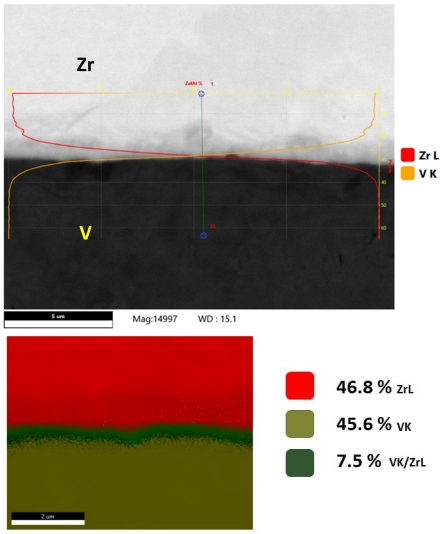

Figure 6: SEM image and EDS line scan (top) and elemental dot map (bottom) of the interface area between V and Zr.

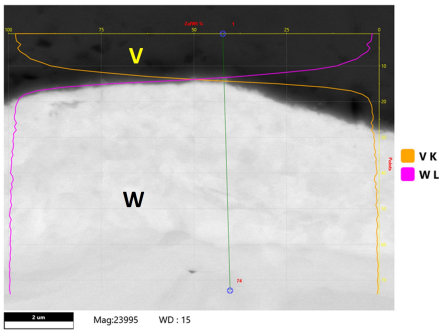

Figure 7: SEM image and EDS line scan of the interface area between V and W.

pressure was held for 2 hours duration. The diffusion depth of the V and W bonding region was about 1 µm showing a smooth elemental transition from the W to V. The interaction zone between the V and Zr was also about 1 µm. In the bonding region, the elemental mixture was about 50:50 for V and Zr. This indicates that the VHP applied condition was enough to form diffusion bonding between V and Zr, but not enough to make the bonding region reach V-Zr binary alloy equilibrium state, forming a brittle ZrV_2 intermetallic layer. These observations show the feasibility of cladding tungsten with zirconium alloys by applying vanadium foil inter layer. Zirconium alloys and vanadium are low activation materials compared to tantalum. This opens a way to develop a water-cooled tungsten target that is subject to low decay heat, which will allow higher proton beam power on the target from a safety hazard perspective in LOCA.

ACKNOWLEDGMENTS

We thank D. Newberry, S. Reeves and T. Lowe for assistance with VHP, Metallography and SEM.

Content from this work may be used under the terms of the CC BY 4.0 licence (© 2024). Any distribution of this work must maintain attribution to the author(s), title of the work, publisher, and DOI.

ISBN: 978-3-95450-247-9 ISSN: 2673-5490 doi: 10.18429/JACoW-IPAC2024-THPS44

© Content from this work may be used under the terms of the CC BY 4.0 licence (© 2024). Any distribution of this work must maintain attribution to the author(s), title of the work, publisher, and DOI.

REFERENCES

[1] A. T. Nelson, J. A. O'Toole, R. A. Valicenti, and S.A. Maloy, "Fabrication of a tantalum-clad tungsten target for LANSCE", *J. Nucl. Mater.*, vol. 431, pp. 172–184, 2012. doi:10.1016/j.jnucmat.2011.11.041.

[2] J. W. G. Thomason, "The ISIS Spallation Neutron and Muon Source—The first thirty-three years", *Nucl. Instrum. Methods Phys. Res. Sect. A*, vol. 917, pp. 61–67, 2019. doi:10.1016/j.nima.2018.11.129

[3] S. Wei *et al.*, "Overview of CSNS tantalum cladded tungsten solid Target-1 and Target-2", *Nucl. Eng. Technol.*, vol. 54, pp. 1535–1540, 2022. doi:10.1016/j.net.2021.10.032

[4] J. Chen *et al.*, "Mechanical properties of pure tantalum after 800 MeV proton irradiation", *J. Nucl. Mater.*, vol. 298, pp. 248–254, 2001. doi:10.1016/S0022-3115(01)00654-7

[5] S. Saito, K. Suzuki, H. Obata, and Y. Dai, "Mechanical properties of pure tungsten and tantalum irradiated by protons and neutrons at the Swiss spallation-neutron source," *Nucl. Mater. Energy*, vol. 34, 101338, 2023. doi.org/10.1016/j.nme.2022.101338.

[6] T. A. Broome, "PROSPECTS FOR TARGETS AND METHANE MODERATORS AT ISIS", in *Proc. ICANS-XII, 13th Meeting of the International Collaboration on Advanced Neutron Sources*, Paul Scherrer Institut, 5232 Villigen PSI, Switzerland, Oct. 1995.

[7] Y. Lee, "Proton beam power limits for stationary water-cooled tungsten target with different cladding material options", presented at IPAC'24, May 19-24, 2024, Nashville, Tennessee, USA, 2024.

[8] G. A. Greene and C. C. Finfrock, "Vaporization of tungsten in flowing steam at high temperatures", *Expe. Therm. Fluid Sci.*, vol. 25, no. 3–4, pp. 87–99, Oct. 2001. doi:10.1016/S0894-1777(01)00063-2

[9] M. Kawai, S. Ikeda, and T. Ino, "KENS-II, its History from Design to Removal", *Mater. Sci. Forum*, vol. 1024, pp. 13–26, 2021. doi:10.4028/www.scientific.net/MSF.1024

[10] J. M. Carpenter and A. G. Hins, "EXPERIENCE WITH IPNS TARGETS", in *Proc. ICANS XII*, Abingdon, UK, May 24–28, 1993.

[11] W. Wagner, "Target operation at the high-power neutron spallation source SINQ: Safety and reliability issues", in *Proc. Workshop on Radiation Protection Issues Related to Radioactive Ion-Beam Facilities (SAFERIB)*, CERN, Geneva, Switzerland, 30 Oct–1 Nov 2002, pp. 15–25, 2022.

[12] Y. Xu, J. Zhang, and H. Li, "Rudimentary investigation of the HIP process for tungsten target", *J. of Nucl. Mater.*, vol. 377, pp. 97–100, 2008. doi:10.1016/j.jnucmat.2008.02.052

[13] Y.-I. Jung *et al.*, "HIP Joining of Tungsten Armor to Ferritic-Martensitic Steel with a Zirconium Interlayer", *Fusion Science and Technology*, vol. 72:3, pp. 523–529, 2017. doi.org/10.1080/15361055.2017.1330610

[14] K. Wang, X. Liu, T. Liu, C. He, and J. Liu, "Interdiffusion in Zr-Mo/W Intermetallics", *Appl. Sci.*, vol. 13, p. 6375, 2013. doi.org/10.3390/app13116375